The EMBO Journal (2011) 30, 1690–1704 | © 2011 European Molecular Biology Organization | Some Rights Reserved 0261-4189/11
www.embojournal.org

THE EMBO JOURNAL

EMBO open

Regulation of interkinetic nuclear migration by cell cycle-coupled active and passive mechanisms in the developing brain

Yoichi Kosodo[1,2,*], Taeko Suetsugu[1], Masumi Suda[2], Yuko Mimori-Kiyosue[3], Kazunori Toida[2], Shoji A Baba[4], Akatsuki Kimura[5] and Fumio Matsuzaki[1,*]

[1]Laboratory for Cell Asymmetry, RIKEN Center for Developmental Biology, Kobe, Japan, [2]Department of Anatomy, Kawasaki Medical School, Kurashiki, Japan, [3]Optical Image Analysis Unit, RIKEN Center for Developmental Biology, Kobe, Japan, [4]Department of Biology, Ochanomizu University, Tokyo, Japan and [5]Cell Architecture Laboratory, Center for Frontier Research, National Institute of Genetics, Shizuoka, Japan

A hallmark of neurogenesis in the vertebrate brain is the apical–basal nuclear oscillation in polarized neural progenitor cells. Known as interkinetic nuclear migration (INM), these movements are synchronized with the cell cycle such that nuclei move basally during G1-phase and apically during G2-phase. However, it is unknown how the direction of movement and the cell cycle are tightly coupled. Here, we show that INM proceeds through the cell cycle-dependent linkage of cell-autonomous and non-autonomous mechanisms. During S to G2 progression, the microtubule-associated protein Tpx2 redistributes from the nucleus to the apical process, and promotes nuclear migration during G2-phase by altering microtubule organization. Thus, Tpx2 links cell-cycle progression and autonomous apical nuclear migration. In contrast, *in vivo* observations of implanted microbeads, acute S-phase arrest of surrounding cells and computational modelling suggest that the basal migration of G1-phase nuclei depends on a displacement effect by G2-phase nuclei migrating apically. Our model for INM explains how the dynamics of neural progenitors harmonize their extensive proliferation with the epithelial architecture in the developing brain.

The EMBO Journal (2011) **30,** 1690–1704. doi:10.1038/emboj.2011.81; Published online 25 March 2011
Subject Categories: cell & tissue architecture; development
Keywords: cell cycle; computational model; microtubule; neuroepithelial cell; Tpx2

*Corresponding authors. Y Kosodo, Department of Anatomy, Kawasaki Medical School, 577 Matsushima, Kurashiki 701-0192, Japan. Tel.: +81 86 462 1111; Fax: +81 86 462 1199;
E-mail: kosodo@med.kawasaki-m.ac.jp or F Matsuzaki, Laboratory for Cell Asymmetry, RIKEN Center for Developmental Biology, 2-2-3 Minatojima-Minamimachi, Chuou-ku, Kobe 650-0047, Japan. Tel.: +81 78 306 3217; Fax: +81 78 306 3215;
E-mail: fumio@cdb.riken.jp

Received: 19 May 2010; accepted: 23 February 2011; published online: 25 March 2011

Introduction

During vertebrate development, brain tissues must maintain their structure even as they increase in complexity through the proliferation of neural progenitor cells and differentiation of their progeny. The neuroepithelium is polarized, with a basal side and an apical, ventricular surface that abuts the lumen of the neural tube early in development. The neuroepithelial cells, which are highly elongated extending thin processes toward the basal and apical surfaces, initially grow their population through proliferation, and subsequently gives rise to neurogenic progenitor cells that both self-renew and generate neurons (Götz and Huttner, 2005). Proliferation of progenitor cells occurs in the ventricular zone (VZ), the apical-most region of neuroepithelium. Neurons and fate-committed progenitor cells migrate away from the VZ, transforming a single-layered pseudostratified tissue into a multi-layered tissue. Thus, the VZ is maintained as the major germinal layer throughout the enormous expansion of progenitor cells and the extensive production of neurons in brain development. Despite its importance, however, the mechanisms that maintain the VZ structure are not well understood.

Neural progenitor cells in the VZ exhibit interkinetic nuclear migration (INM), in which their nuclei migrate between the apical surface and the basal part of the VZ in synchrony with the cell cycle (see Figure 1A). After mitosis at the apical surface (M-phase), the nuclei migrate basally during G1-phase and subsequently stay at the basal region of the VZ during S-phase. In G2-phase, the nuclei migrate apically, entering M-phase upon reaching the apical surface. This characteristic oscillation of the nuclei of neural progenitor cells was first identified in the embryonic neuroepithelium more than 70 years ago (Sauer, 1935), and was experimentally verified thereafter (Sauer and Walker, 1959; Fujita, 1960). INM has been observed in other epithelial tissues, including chick basilar papilla (Raphael *et al*, 1994) and embryonic mouse liver buds (Bort *et al*, 2006), suggesting that this process is a hallmark not only of neuroepithelium, but of all pseudostratified epithelia.

Notably, studies using mouse brain and zebrafish retina have suggested that INM is critical for the self-renewal of neural progenitor cells (Xie *et al*, 2007; Del Bene *et al*, 2008; Zhang *et al*, 2009; Taverna and Huttner, 2010). The importance of INM in the developing brain has prompted several attempts to identify underlying mechanisms. One drug treatment study using cell-cycle inhibitors suggested that the cell cycle controls nuclear migration, while nuclear migration does not control the cell cycle (Ueno *et al*, 2006). Previous studies using inhibitors of actin (Messier and Auclair, 1974;

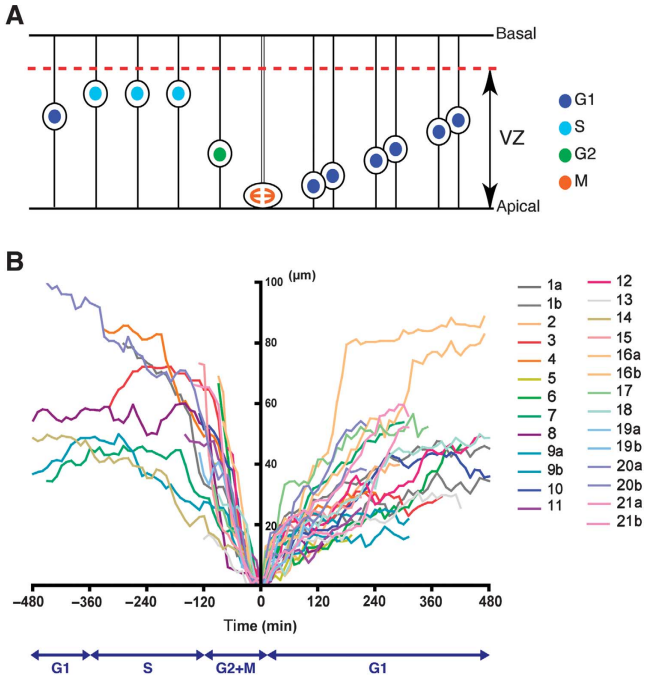

Figure 1 Quantitative tracking of nuclear movement of cortical neural progenitor cells in embryonic mouse brain slice cultures. (**A**) Schematic model of INM of neural progenitor cells. Nuclei in the VZ, the closest tissue layer to the ventral surface of the developing brain, show an oscillatory movement along the apical–basal epithelial axis that is associated with the phase of the cell cycle (see Introduction). The colour code of cell-cycle phases is indicated on the right. (**B**) Representative movement of a nucleus undergoing INM. Nuclei of neural progenitor cells were labelled by NLS-GFP, and their movements in slice cultures prepared from E13.5 mouse brains were tracked by time-lapse microscopy. Using the tracking software, positions of nuclei from the apical surface (*y*-coordinate) were measured according to their incubation time (*x*-coordinate). The time point at which nuclei showed the most apical localization was defined as zero. Phases of the cell cycle, estimated from previous reports, are indicated below (see Results). Numbers and colour codes of nuclei are indicated on the right (a or b after the numbers indicate daughter cells derived from cell division at the apical surface).

Murciano *et al*, 2002) or microtubules (Messier, 1978) suggest that proper cytoskeletal organization is either directly or indirectly necessary for INM. Indeed, it has been suggested that INM is perturbed by eliminating the activity of several molecules with putative functions in cytoskeletal regulation, including β-catenin (Machon *et al*, 2003), Cdc42 (Cappello *et al*, 2006), gap-junction proteins (Pearson *et al*, 2005), the serine/threonine kinase CK2 (Carneiro *et al*, 2008), Rac (Minobe *et al*, 2009), Myosin II (Norden *et al*, 2009) and Laminin (Tsuda *et al*, 2010). Components of microtubule-based dynein motor complex, such as Lis1 (Tsai *et al*, 2005) and dynactin (Del Bene *et al*, 2008), and centrosomal activity at the apical surface (Tamai *et al*, 2007; Xie *et al*, 2007), have been clearly shown to be involved in basal-to-apical nuclear migration. The connection between dynein and the nuclear envelope is maintained by SUN-domain proteins and KASH-domain proteins; loss of their molecular function impairs INM (Del Bene *et al*, 2008; Zhang *et al*, 2009). Thus, it is likely that basal-to-apical nuclear migration is actively driven by microtubule-based motors and is therefore cell autonomous. However, cell cycle-dependent expression has not been reported for known molecular drivers of basal-to-apical nuclear migration, and it remains unexplained why this movement occurs during G2-phase.

In the present study, we sought to address a pair of questions that must be answered before a comprehensive model of INM can be developed. Namely, what mechanisms couple the timing and direction of nuclear movement with cell-cycle progression in neural progenitor cells, and how is apical-to-basal migration achieved? Recent reports demonstrate that the actomyosin system (Schenk *et al*, 2009) or kinesin-type microtubule plus-end-directed motors (Tsai *et al*, 2010) are involved in carrying nucleus from the apical region to the basal region of the VZ, although mechanisms by which such cytoskeletal motors act in G1-phase are not addressed. We here report that the basal-to-apical migration of neural progenitor cells that occurs in INM is regulated by Tpx2, a microtubule-associated protein (Gruss *et al*, 2001; Schatz *et al*, 2003). Tpx2 is localized to apical processes during G2-phase and alters microtubule organization in a cell cycle-dependent manner. Moreover, we show by *in situ* experiments and computational modelling that the apical-to-basal migration of nuclei in G1-phase occurs mainly through passive, non-autonomous displacement, which we ascribed to the autonomous nuclear movement of G2-phase nuclei moving in the opposite direction. The resulting model of INM describes a mechanism for VZ tissue homeostasis coordinated with progenitor cell proliferation.

Results

Nuclei of neural progenitor cells show characteristic movement depending on the phase of the cell cycle

To analyse nuclear movement during INM, we established a system that enabled us to quantitatively track the motion of individual nuclei in living tissue. Nuclei in the dorsal cortex of an E13.5 mouse brain were labelled by green fluorescent protein (GFP) containing a nuclear localization signal (NLS)

using *in utero* electroporation. Labelled nuclei in cultures of brain slices were tracked using a video imaging system (Supplementary Movie S1), and their location at each time frame was plotted (Figure 1B). After mitosis at the apical surface (time point = 0 in Figure 1B), nuclei migrate basally within the VZ. Before mitosis, nuclei migrate apically. Using previous studies that measured the length of the cell cycle in neural progenitor cells (Takahashi *et al*, 1995), we were able to correlate the position of tracked nuclei during INM with phases of the cell cycle (Figure 1B). In this way, we confirmed the basic scheme of INM described previously (Sauer, 1935; Sauer and Walker, 1959; Fujita, 1960), suggesting that our experimental set-up faithfully represented *in vivo* neural progenitor dynamics. Analysis of the kinetics of INM identified three novel features of nuclear movement. First, nuclear 'ratcheting', a forward and backward motion of nuclei, occurs while the nuclei migrate toward the basal side during G1-phase (after 0 min in Figure 1B). Second, during the basal-to-apical migration before mitosis (G2-phase, around −120 to 0 min in Figure 1B), the nuclei show linear movements and faster kinetics than nuclei that are moving in the opposite direction. Third, the individual positions of nuclei within the population differ remarkably before they begin basal-to-apical migration (during S-phase, before −120 min in Figure 1B). Furthermore, some nuclei show slow basal-to-apical migration during S-phase, although most remain stationary. These features of S-phase nuclei have been indicated by other reports using histological methods (Takahashi *et al*, 1993; Hayes and Nowakowski, 2000), suggesting that they are not artifacts of our experimental system.

Molecular evidence for the cell cycle dependence of INM

Individual phases of INM are tightly correlated with phases of the cell cycle, but it has not been determined how migration depends on cell-cycle progression. To address this question, we first examined whether INM depends on G1- to S-phase progression. The cell cycle of neural progenitors was arrested at G1-phase by overexpression of $p18^{Ink4c}$, a cyclin-dependent kinase inhibitor (Guan *et al*, 1994; Sherr and Roberts, 1999). Introduction of $p18^{Ink4c}$ by *in utero* electroporation resulted in a decrease in the number of cells expressing Ki67, a marker for the proliferative state (Figure 2A). The electroporated cells were neither labelled by BrdU, which is incorporated into DNA during S-phase (Supplementary Figure S1A), nor observed histologically to be in M-phase. These cells, therefore, had passed through M-phase and were arrested in G1-phase by the time of analysis (18 h after electroporation). Interestingly, at E10.5, when proliferative cells are dominant, the cell bodies of the $p18^{Ink4c}$-electroporated cells accumulated in the basal region of the VZ, with their long apical processes extended toward the apical surface (Figure 2B). This phenomenon is not specific to this developmental stage, as statistical measurements showed basal accumulation of G1-arrested nuclei in the VZ at E14.5 as well (Figure 2C and D). The basal nuclear localization of $p18^{Ink4c}$-expressing cells may be due to differentiation of G1-arrested progenitor cells into neurons that do not migrate to the apical surface. However, we confirmed that the progenitor state is not affected in $p18^{Ink4c}$-expressing cells based on expression of Sox2 (Supplementary Figure S1B) and Pax6 (Supplementary Figure S1C), markers for apical neural progenitor cells (Götz *et al*, 1998; Graham *et al*, 2003). Furthermore, we did not observe any significant changes in the pattern of Tuj1 staining, a marker for neurons, nor any increase in expression of Tbr2, a marker for differentiating intermediate progenitor cells (Kowalczyk *et al*, 2009), 24 h after electroporation (Supplementary Figure S1D and E). These results indicate that the nuclei of neural progenitor cells do not migrate in the apical direction when they are arrested in G1-phase and suggest that entry into S-phase is a prerequisite for basal-to-apical nuclear migration.

Tpx2, a microtubule-associated protein, regulates basal-to-apical nuclear migration during G2-phase

The dependence of basal-to-apical migration on both cell-cycle progression (Figure 2) and microtubules (Supplementary Figure S2; Supplementary Movie S2; Tsai *et al*, 2005; Xie *et al*, 2007) indicates that microtubule regulation coupled with the cell cycle might control the timing of nuclear migration. Based on reports from other studies (Gruss *et al*, 2002; Schatz *et al*, 2003; Gruss and Vernos, 2004), one possible candidate molecule fulfilling this role is Tpx2. Tpx2 is a microtubule-nucleating/bundling protein involved in spindle pole formation around chromosomes dependent on Ran-GTP activity (Gruss and Vernos, 2004). In HeLa cells, Tpx2 protein expression is regulated by the cell cycle; it accumulates in nuclei during S/G2-phase, localizes at the spindle pole during M-phase, and is degraded in early G1-phase (Gruss *et al*, 2002). We first characterized the protein expression pattern of Tpx2 in neural progenitor cells in the embryonic mouse brain. BrdU labelling to identify the phase of the cell cycle (Takahashi *et al*, 1992) showed that Tpx2 is expressed in neural progenitor cells in S-, G2- and M-phases (Figure 3A, open arrowheads). We noted that, in addition to the nuclear staining, Tpx2 was found in a fibre-like pattern within VZ cells (Figure 3Aa, arrows). Introduction of cell cycle phase marker (CCPM; Figure 3Ba; Supplementary Movie S3) into neural progenitor cells showed that these fibre-like structures were located in the apical processes only during G2-phase, and were absent in G1-phase (Figure 3Bb; Supplementary Figure S3A), suggesting that Tpx2 functions in the apical processes of the G2-phase neural progenitor cells. When GFP-tagged Tpx2 was expressed in neural progenitor cells, GFP-Tpx2 specifically localized to the nuclei and apical processes of cells in the VZ (Figure 3C). During interphase, GFP-Tpx2 in the apical processes extended toward centrosomes on the apical surface, whereas during M-phase, it was present on mitotic spindles (Supplementary Figure S3B). Co-electroporation of CCPM and 6myc-Tpx2 revealed that the exogenous Tpx2 protein was distributed within the apical processes but never within the basal processes of G2-phase neural progenitor cells (Figure 3D). Ultrastructural analysis using high-voltage electron microscopy (HVEM) showed bundled fibre-like patterns of GFP-Tpx2 reminiscent of microtubule structure within the apical processes (Figure 3E). The microtubule bundling activity of Tpx2 had been previously shown in a purified *in vitro* system (Schatz *et al*, 2003), and when taken together, our results strongly suggest that Tpx2 is associated with microtubules in the apical processes of neural progenitor cells. Furthermore, even though both the basal and apical processes of these cells contain large amount of microtubules, the localization of Tpx2 is restricted to the apical processes, suggesting that

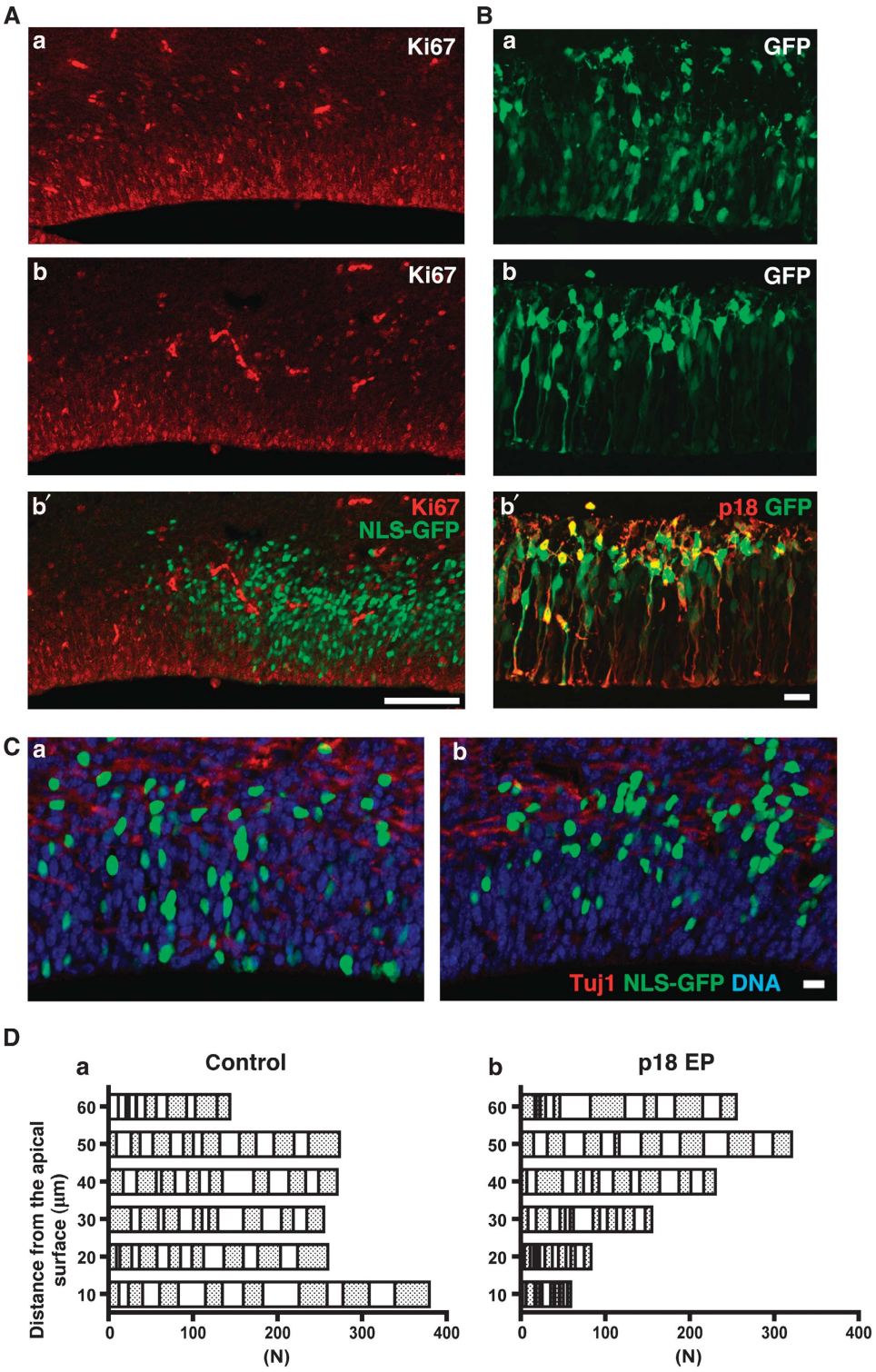

Figure 2 Arresting the cell cycle in G1-phase by introduction of $p18^{Ink4c}$ induces accumulation of nuclei in the basal region of the VZ. (**A**) Immunostaining of E14.5 mouse brain treated with $p18^{Ink4c}$ to arrest the cell cycle in G1-phase with a Ki67 antibody (proliferative marker, red). (a) Contralateral side. (b, b′) E13.5 mouse lateral cortex in which $p18^{Ink4c}$ (b) and NLS-GFP (b′; green) were co-electroporated and incubated for 24 h. Bar = 50 μm. (**B**) Expression of GFP (green) with electroporation of either control vector (a) or $p18^{Ink4c}$ (b, b′) into E10.5 mouse telencephalon followed by 18 h of whole-embryo culture. Immunostaining using a $p18^{Ink4c}$ antibody was performed (b′; red). Bar = 10 μm. (**C**) Positions of NLS-GFP-expressing nuclei with control vector (a) or $p18^{Ink4c}$ (b) introduced by electroporation into E13.5 mouse cortex followed by a 24-h incubation. Co-staining using a Tuj1 antibody (neuronal marker, red) and DAPI (DNA, blue) was performed. Bar = 10 μm. (**D**) Positions of NLS-GFP-expressing nuclei relative to the apical surface with control vector (a) or $p18^{Ink4c}$ (b). Sums of numbers (*N*, *x*-coordinate) counted in 15 electroporated brain sections (nuclei from each section are indicated by white or dotted boxes) are shown according to their distance from the apical surface (*y*-coordinate). For (**A**–**C**), apical surface is down.

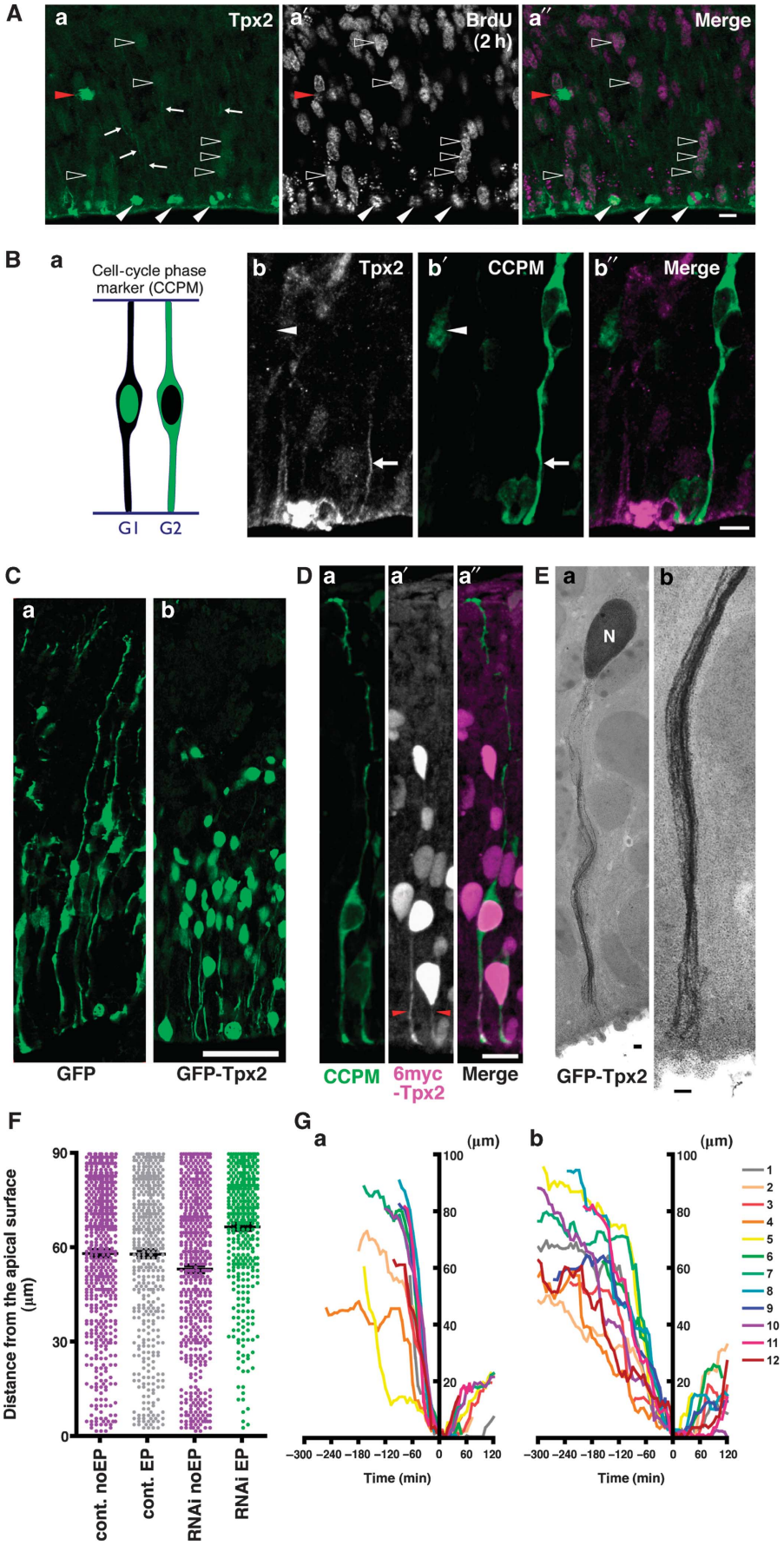

its association with microtubules is not promiscuous (Supplementary Figure S3C).

Basal-to-apical nuclear migration is correlated with Tpx2-dependent microtubule organization in the apical process in G2-phase

We next examined whether Tpx2 is involved in basal-to-apical nuclear migration by reducing its activity using a vector-based RNA interference (RNAi) approach. The protein level of Tpx2 was significantly decreased by the RNAi treatment; the treatment eventually induced mitotic arrest 24 h after electroporation (Supplementary Figure S4A) and abolished mitotic spindles (Supplementary Figure S4B), as in the case of HeLa cells (Gruss *et al*, 2002). To examine the effect of *TPX2* RNAi treatment on INM, we first examined the positions of BrdU-containing cells in the VZ. After BrdU incorporation in S-phase, BrdU-labelled nuclei migrated toward the apical surface during incubation for 90 min (Figure 3F, cont. EP). We observed that this nuclear migration activity was significantly decreased with a knockdown of *TPX2* (Figure 3F, RNAi EP). Non-electroporated cells in the same area did not show a decrease in this migration activity (Figure 3F, RNAi noEP), suggesting that this aspect of nuclear migration is perturbed cell autonomously. We confirmed that *TPX2*-RNAi did not result in an increase of apoptotic cells with the 18-h time course of the experiment (Supplementary Figure S4C), and that the perturbed basal-to-apical nuclear migration by *TPX2*-RNAi was recovered by introduction of the human *TPX2* gene (Supplementary Figure S4D). Similar perturbed nuclear movement was also observed using RNAi with a different target sequence (Supplementary Figure S5A), indicating that the perturbation in nuclear migration by *TPX2* knockdown was not due to an off-target effect of RNAi. More directly, we analysed the dynamics of basal-to-apical nuclear migration in brain slices treated with *TPX2* RNAi and observed (1) a decrease in velocity of migration and (2) a non-linear, stepwise movement during migration (Figure 3G; Supplementary Movies S4 and S5). When *TPX2* is knocked down, the average velocity of nuclear movement from basal-to-apical region (50–15 μm from the apical surface, respectively) showed a statistically significant decrease (Figure 3G, from 1.0 ± 0.11 (control) to 0.5 ± 0.07 (*TPX2* RNAi) μm/min, *P*-value < 0.001, *t*-test). In addition, the number of subapical mitotic cells was increased in the *TPX2* RNAi-treated brain, suggesting that the nuclei had entered M-phase before reaching the apical surface (Supplementary Figure S5B). This can be attributed to slower nuclear movement in the apical direction. Taken together, these results suggest that the expression of Tpx2 during G2-phase is necessary to regulate proper nuclear migration from the basal-to-apical region of the VZ.

We next sought to elucidate how Tpx2 affects G2-phase nuclear migration. *TPX2* RNAi might affect epithelial polarity or centrosomal activity; however, we did not find any aberrant pattern using markers of epithelial characteristics such as ZO-1, Par-3 and β-catenin or using a marker for TACC3, a centrosomal protein involved in INM (Xie *et al*, 2007), in the *TPX2* knocked-down tissue (Supplementary Figure S5C–E). We then tested the possibility that microtubule organization in the apical processes of neural progenitor cells is regulated by Tpx2 in a cell cycle-dependent manner. To visualize microtubule organization at specific cell-cycle stages, we introduced fluorescence-tagged EB3, a microtubule plus-end-binding protein (Mimori-Kiyosue and Tsukita, 2003) and CCPM to neural progenitor cells in the developing brain (Figure 4A). Live imaging of EB3-tagRFP characterized 'comet-like' movement of the protein (Supplementary Movie S6), as reported in a previous study of migrating neurons (Tsai *et al*, 2007), indicating that the expression level of EB3-tagRFP is moderate in our system. Because we noticed that chemical fixation with paraformaldehyde or methanol disrupted EB3 localization in tissue (data not shown), we observed signals of EB3-tagRFP and CCPM in living brain slices. In controls, we found that EB3 signals were more sharply distributed inside the apical process in G2-phase than in G1-phase (Figure 4Bab and Cb). By contrast, in the *TPX2* knocked-down cells, the profile of EB3 signals during both G1- and G2-phases was essentially indistinguishable from that in normal G1-phase cells (Figure 4Cb), indicating that the sharpened microtubule distribution in the G2-phase apical process requires Tpx2. Given that Tpx2 functions to bundle purified microtubules (Schatz *et al*, 2003), Tpx2 is likely to alter microtubule organization in the apical process of G2-phase cells during the S to G2 progression. While Tpx2

Figure 3 Tpx2 shows temporal expression and association with microtubules in neural progenitor cells, and loss of Tpx2 function perturbs basal-to-apical nuclear migration. (**A**) Immunostaining for Tpx2 (a), incorporation of BrdU followed by a 2-h incubation (a′), and the merged view (a″; Tpx2, green; BrdU, magenta) in a cryosection of E14.5 mouse brain tissue. Open arrowheads indicate the Tpx2 and BrdU double-positive cells. Arrows indicate Tpx2 signals outside the nucleus. Note that dividing cells showed strong expression of Tpx2 on their mitotic spindles (white arrowheads, apical mitotic cell; red arrowhead, basal progenitor cell). Bar = 10 μm. (**B**) (a) Schematic showing the cell cycle-dependent translocation of GFP in CCPM-electroporated cells. (b) Co-labelling of E13.5 mouse brain tissue using Tpx2 antibody, CCPM and the merged view (b″; Tpx2, magenta; CCPM, green). The white arrowhead indicates the nucleus of a G1-phase neural progenitor cell, whereas the white arrow indicates the apical process of a G2-phase cell identified by CCPM localization. Bar = 10 μm. (**C**) Expression of GFP (a) or GFP-Tpx2 (b) in neural progenitor cells in E13.5 mouse brain tissue. Note that GFP-Tpx2 localizes to nuclei and apical processes extended in the VZ but not to basal processes. Bar = 50 μm. (**D**) Co-expression of CCPM (a), 6myc-TPX2 (a′) and the merged view (a″; CCPM, green; 6myc-Tpx2, magenta). Red arrowheads in (a′) indicate 6myc-Tpx2 localization at apical processes. Bar = 10 μm. (**E**) HVEM image of GFP-Tpx2 in neural progenitor cells. (a, b) A plasmid encoding GFP-Tpx2 was electroporated into E12.5 mouse brain tissue and incubated for 24 h before dissection. Immunostaining using gold particles was performed on vibratome sections, followed by specimen preparation for HVEM analysis. Note the gold particles localized within the nucleus (a) and on several fibre-like structures in the apical processes (a, b). N, nucleus. Bars = 1 μm. (**F**) Nuclear positions after BrdU incorporation in S-phase followed by a 1-h or 30-min incubation with LacZ miR RNAi as a control (cont., grey dots) or Tpx2 miR RNAi (RNAi, green dots) in E13.5 mouse brain tissue. *y*-coordinate: distance from apical surface (below 90 μm), EP: NLS-GFP-positive nuclei (electroporated cells), noEP; NLS-GFP-negative nuclei in the same microscopic frame (magenta dots). Black error bars indicate standard error of the mean (s.e.m.). (**G**) Tracking of basal-to-apical nuclear movement with LacZ miR RNAi as a control (a) or Tpx2 miR RNAi (b) in slice cultures prepared from E13.5 mouse brain tissue. Positions of nuclei relative to the apical surface (*y*-coordinate) were measured according to their incubation time (*x*-coordinate). The time point at which nuclei showed the most apical localization was defined as zero. Numbers and colour codes of nuclei are indicated on the right. For (**A**–**E**), apical surface is down.

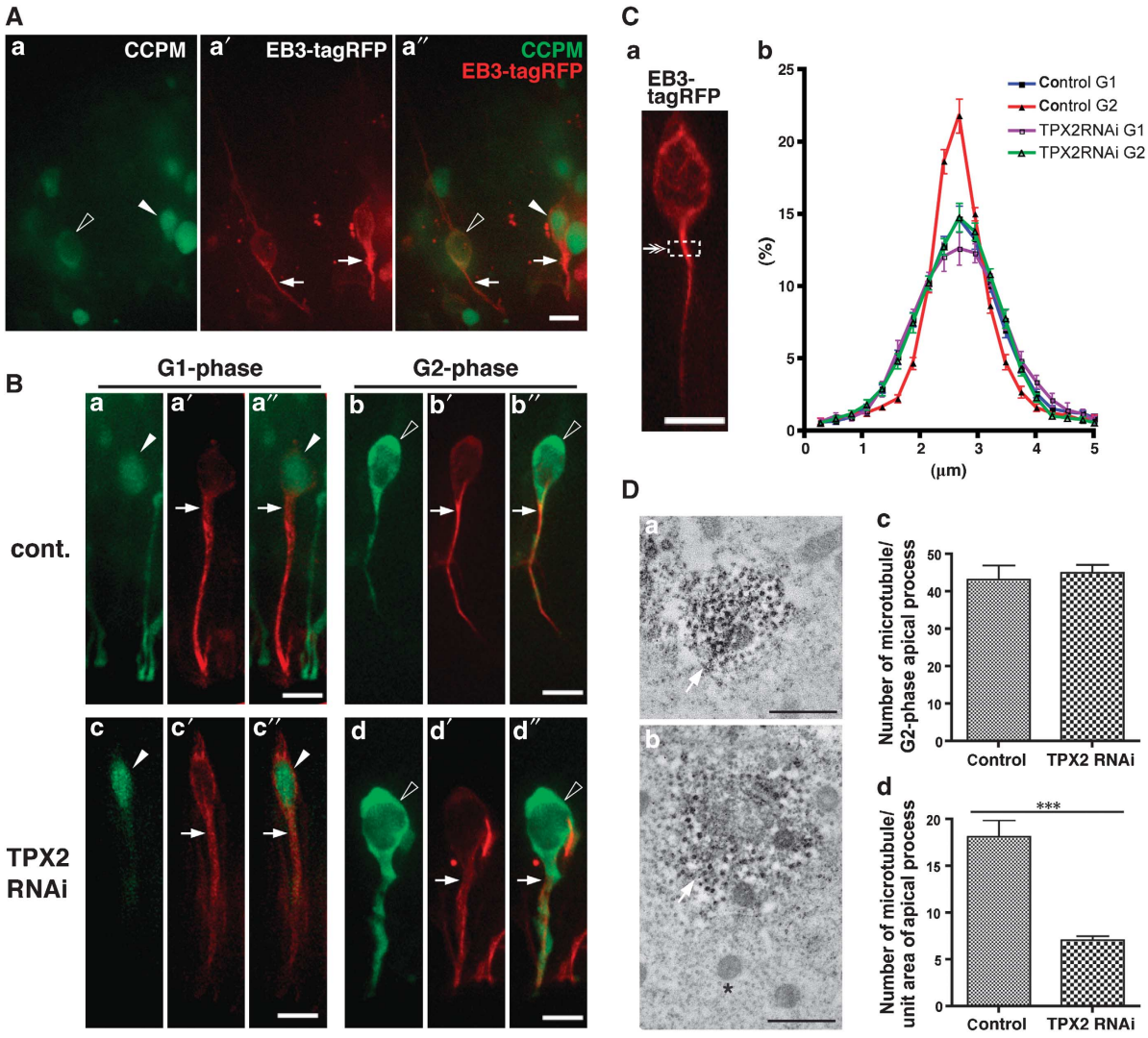

Figure 4 Tpx2 alters microtubule organization in the apical process of G2-phase neural progenitor cells. (**A**) Images of cell cycle phase marker (CCPM; a) and EB3-tagRFP (a′) in living brain slice cultures. CCPM and EB3-tagRFP were co-electroporated into neural progenitor cells in E12.5 mouse brain, and fluorescent signals from two separate wavelengths were acquired from living tissue slices prepared from E13.5 brain. Note that CCPM localization inside the nucleus indicates that the cell is in G1-phase (filled arrowhead in a and a″), whereas its localization peripheral to the nucleus indicates that the cell is in G2-phase (open arrowhead in a and a″). Arrows in a′ and a″ indicate organizations of microtubules in the apical process identified by EB3-tagRFP. (**B**) Examples of microtubule organization in each cell-cycle phase combined with knockdown of Tpx2 functions. Images were acquired as described in (**A**). LacZ miR RNAi (control, a, b) or Tpx2 miR RNAi (c, d) were co-electroporated together with CCPM and EB3-tagRFP. Cell-cycle phases identified by the localization of CCPM are indicated in the panel. Arrowheads and arrows are as described in (**A**). (**C**) Quantitation of EB3-tagRFP in the apical process. (a) Scanning of EB3-tagRFP signal in the apical process. The pixel intensity of tagRFP fluorescence in the region of the apical process close to the nucleus (dotted rectangle, 5 μm in length) was measured using MetaMorph software. The double arrow indicates the direction of scanning. (b) Relative intensity of EB3-tagRFP fluorescence in each cell-cycle phase combined with knockdown of Tpx2 functions. The pixel intensity of tagRFP fluorescence in each condition (colour codes are indicated in the panel) was quantified as described in (a). Signals were normalized as follows: after subtracting the background level from the raw digitized value of pixel intensity, the remaining value was divided by the sum of all the background-corrected values to calculate percentages (*y*-coordinate). Error bars indicate s.e.m. Bars in (**A**–**C**) = 10 μm. (**D**) Ultrastructural analysis of Tpx2 function on microtubule organization. LacZ miR RNAi (control, a) or Tpx2 miR RNAi (b) were co-electroporated together with CCPM into neural progenitor cells in E13.5 mouse brain, and a slice culture was prepared. After the fixation and permeabilization, pre-embed immunolabelling (Toida *et al*, 2000) was performed on the brain slice using GFP antibody and 3,3′-diaminobenzidine (DAB) reaction to identify the apical process of G2-phase cells. After embedding, 50-nm thick ultrathin sections parallel to the apical surface were prepared to observe the cross-sections of the apical process (10–15 μm away from the apical surface). Asterisk in (b) show DAB-negative cell, its microtubules are seen as small dots. Note that DAB precipitation around microtubules is distinct in DAB-positive cells (arrows in a, b). Bar = 500 nm. (c, d) Number of microtubules in a single (c) or unit area (0.1 μm^2) (d) of the cross-sections of DAB-positive apical process in control or Tpx2 knocked-down situation (eight cases in each condition). ***$P<0.001$, *t*-test (in d). Error bars indicate s.e.m. For (**A**–**C**), apical surface is down.

might affect microtubule orientation, the resolution of our assay system could not distinguish differences of EB3 movements in the thin process of neural progenitors between *TPX2* knocked-down cells and control cells.

We further explored the role of Tpx2 in the apical process during G2-phase cells by performing immunoelectron microscopy to observe the microtubule organization at ultrastructural resolution in the cross-section of the apical process.

In electron micrographs, the apical process of G2-phase cells, which had been electroporated with CCPM, was recognized by the dark precipitation of DAB when immunostaining of GFP was detected by the DAB-peroxidase reaction (Figure 4D). Microtubules, which were clearly detected by a heavy DAB precipitation, were highly packed in the apical process of G2-phase cells in the control situation (Figure 4Da). When Tpx2 was knocked down (Figure 4Db), the number of microtubules in the cross-section of a DAB-positive (i.e. G2-phase) apical process was nearly equal to that in the control (Figure 4Dc, 43.0 ± 3.8 (control) or 45.0 ± 2.1 (*TPX2* RNAi)), but their density in the unit area ($0.1\,\mu m^2$) of apical process was drastically decreased (Figure 4Dd, 18.1 ± 18 (control) or 7.1 ± 0.5 (*TPX2* RNAi)), indicating that Tpx2 facilitates microtubule packing in the apical process of G2-phase cells. Evaluated together, our results imply that basal-to-apical nuclear migration in the G2-phase requires Tpx2-dependent reorganization of apical microtubules during the G2-phase.

Incorporated microbeads exhibit unidirectional translocation toward the basal region of the VZ

The basal accumulation of G1-arrested nuclei (Figure 2) suggests that neural progenitor cells overexpressing $p18^{Ink4c}$ migrate basally after mitosis at the apical surface under conditions in which surrounding cells undergo normal INM. This raised the possibility of a specific mechanism that conveys nuclei from the apical to the basal region. To test whether the translocation system in the VZ is cell autonomous or dependent on the activity of surrounding cells, we observed the behaviour of fluorescent microbeads in cultures of brain slices. Magnetic fluorescent beads were incorporated into the VZ from its apical surface by applying a magnet on the pial side, followed by brain slice culture and time-lapse imaging (Figure 5A). Incorporated fluorescent beads were initially aligned on the apical surface. Some beads were translocated to the basal region over the course of brain slice culture (Figure 5B). HVEM imaging confirmed that this treatment did not impair normal cell–cell contact or disrupt normal tissue architecture (Supplementary Figure S6). Once introduced, the beads tended to stay at the apical surface for a short time before beginning basally directed translocation (Figure 5C, see Supplementary Movie S7). During the translocation, beads showed 'ratcheting,' back-and-forth movement as observed in the migration of G1-phase nuclei (Figure 1B). Upon reaching the basal region of the VZ, the fluorescent beads terminated their translocation and never entered the neuronal layer (Figure 5D). In addition and importantly, once the beads reached the basal end of the VZ, they remained stationary and did not show the return, basal-to-apical movement (Figure 5C). We then examined whether the basal translocation of beads was due to their association with nuclei migrating in the apical-to-basal direction. A comparison of the trajectories of NLS-GFP-labelled nuclei and fluorescent beads in the same brain slices (Supplementary Movie S8) clearly indicates that nuclei underwent radial migration within the elongated cell shape, whereas beads took more variable orientations (Figure 5E). This result implies that beads move not by adhesion to migrating nuclei. We thus conclude that there is a mechanism by which beads translocate from the apical surface to the basal region through intercellular space in the VZ.

S-phase arrest of neural progenitor cells perturbs apical-to-basal nuclear migration in G1-phase

Microbead translocation in the brain slice suggests that G1-nuclei are driven in the apical-to-basal direction by a non-autonomous mechanism. However, such a mechanism is not immediately apparent. One possibility is that active basal-to-apical migration of nuclei increases the nuclear density high on the apical side of the VZ. The resultant close packing of nuclei may crowd out free nuclei that have completed mitosis, so that they are pushed further away from the ventricular surface. If this is the case, apical-to-basal migration should be affected by the acute perturbation of basal-to-apical migration of nuclei in G2-phase. To test this hypothesis, we arrested the cell cycle at S-phase by drug treatment and performed time-lapse observations of migrating nuclei. We first searched for an appropriate inhibitor to arrest the cell cycle of neural progenitor cells in the mouse brain slice culture in S-phase. Hydroxyurea (HU), which selectively inhibits ribonucleoside diphosphate reductase (Wright *et al*, 1990), leads to a dose-dependent reduction in the number of mitotic cells in the VZ (Figure 6A) without inducing apoptosis below 1 mM (Supplementary Figure S7A). As previously reported in chick neuroepithelium (Murciano *et al*, 2002), we confirmed that HU treatment results in an accumulation of S-phase neural progenitor cells by measuring the rate of BrdU incorporation in nuclei immediately after washing out the HU (Supplementary Figure S7B). The results indicated that the G1–S transition was not impaired by HU treatment. We tracked nuclear movement under these conditions in slice cultures to see the effect of HU administration (Figure 6B; Supplementary Movies S9 and S10). In the presence of HU, the number of apically migrating nuclei was dramatically decreased and S-phase nuclei accumulated in the basal region of the VZ. This result was expected, as HU arrests progenitor cells at S-phase, preventing entry into G2-phase. Time-lapse observations revealed that apical-to-basal migration was also quickly perturbed by HU treatment (Figure 6B and C). Under this condition, the average velocity of nuclei moving in the basal direction was significantly decreased (Figure 6Cd). We did note a few rapidly moving unidentified nuclei (3/42 cases with HU, Figure 6C); however, the majority were impeded. This acute delay in apical-to-basal migration is most likely due to the lack of a decrease in basal nuclear density, and of an increase in apical nuclear density, both of which are simultaneously caused by individual nuclei migrating apically in the normal situation. To confirm that the perturbation of basally directed nuclear movement is not due to unexpected effects of HU on G1-phase cells, but instead due to the physical displacement effect, we tested whether microbead translocation (Figure 5) is also perturbed by the same drug treatment. Indeed, most fluorescent beads incorporated from the apical surface translocated shorter distances after treatment with 1 mM HU than in the control (Figure 6D). To further corroborate the nuclear displacement effects, we arrested the cell cycle of a population of cells at G1-phase by introducing $p18^{Ink4c}$ plasmid (see Figure 2), and examined the distribution of pulse-labelled nuclei (by two thymidine analogues: CldU and IdU, see the figure legend), that have not incorporated $p18^{Ink4c}$ plasmid (i.e. not affected by the cell-cycle arrest). When $p18^{Ink4c}$ plasmid was introduced to the surrounding cells, the distribution of CldU

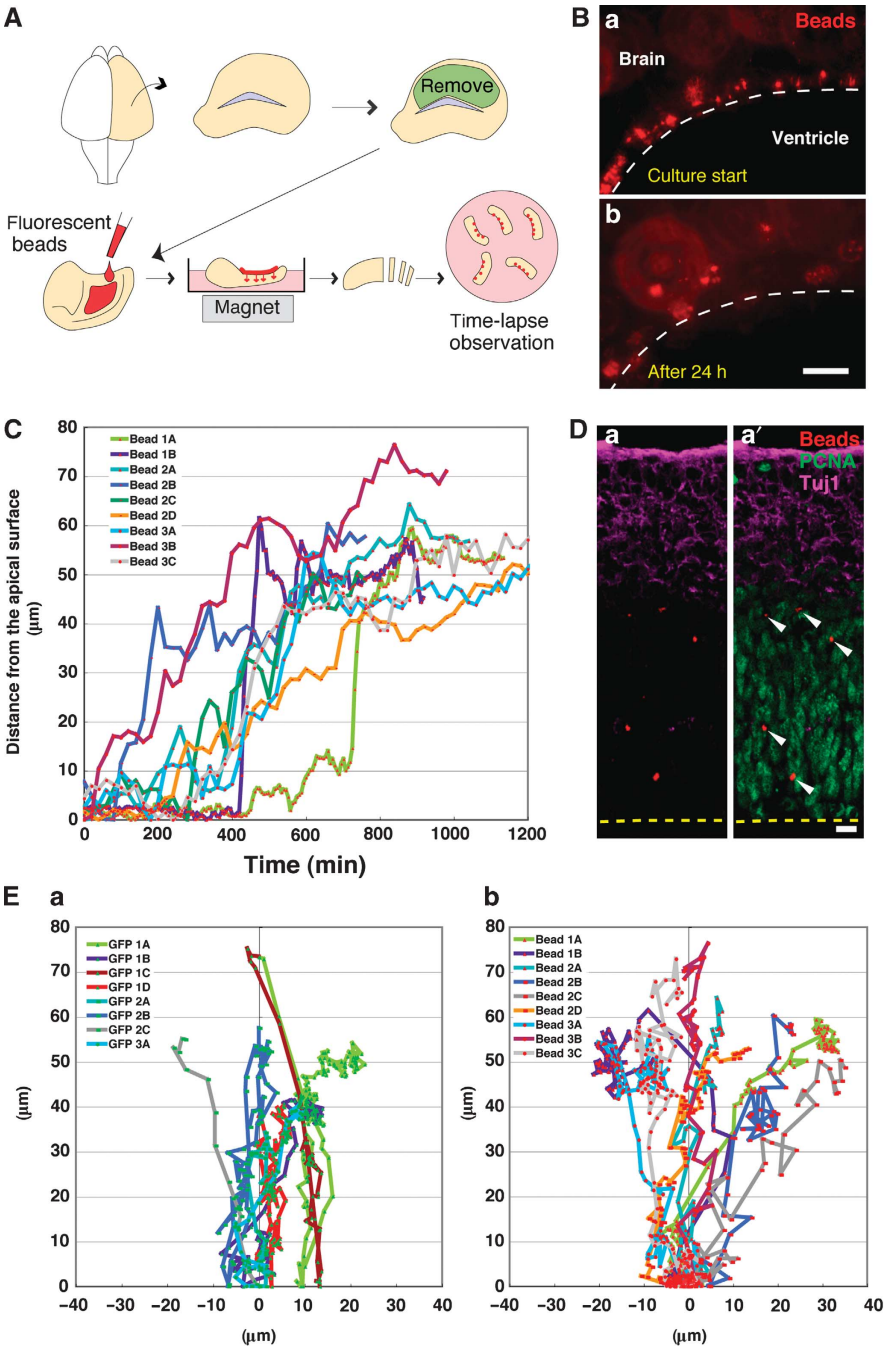

Figure 5 Unidirectional translocation of microbeads from the apical surface toward the basal region of the VZ. (**A**) Schematic of the method used to incorporate fluorescent microbeads (diameters are ~2 μm) into embryonic mouse brain tissue using magnetic activity, followed by tracking of their movement in slice cultures using time-lapse microscopy. (**B**) Images of fluorescent beads in slice cultures (a, b; red) incorporated into E13.5 mouse brain tissue. The white dashed line indicates the apical surface. Beads were aligned at the apical surface at the starting time point (a). Several beads had detached from their original position after 24 h of incubation (b). Bar = 50 μm. (**C**) Tracking of microbeads in brain slice cultures. Positions of fluorescent beads relative to the apical surface (*y*-coordinate) were measured at each time point (*x*-coordinate) from the time-lapse images. Movements of nine microbeads acquired from three independent brain slices are displayed (slice numbers (1–3) and beads (A–D) are indicated in the graph). (**D**) Immunostaining of mouse brain sections from cultured tissue slices after microbead incorporation (a, b; red). Antibody for proliferating cell nuclear antigen (PCNA) stains proliferative cells (a′; green), whereas Tuj1 stains post-mitotic neurons (a, a′; magenta). Note that fluorescent microbeads were observed only in the proliferative zone, the VZ (white arrowheads). Yellow dashed lines indicate the apical surface. Bar = 10 μm. (**E**) Comparison of nuclear and microbead tracks in brain tissue slices. Plane positions of nuclei marked with NLS-GFP (a) or incorporated microbeads (b) were measured along the apical surface (*x*-coordinate) and apical–basal axis (*y*-coordinate). Slice numbers (1–3), nuclei and beads (A–D) are indicated in each graph.

single-labelled nuclei of $p18^{Ink4c}$ plasmid-negative cells showed a notable accumulation close to the apical surface (Figure 6E), indicating that apical-to-basal nuclear migration is perturbed. Based on the results above, we conclude that the apical-to-basal nuclear migration that occurs in G1-phase is subject to a displacement or crowding-out effect of incoming nuclei migrating in the opposite direction after exiting S-phase.

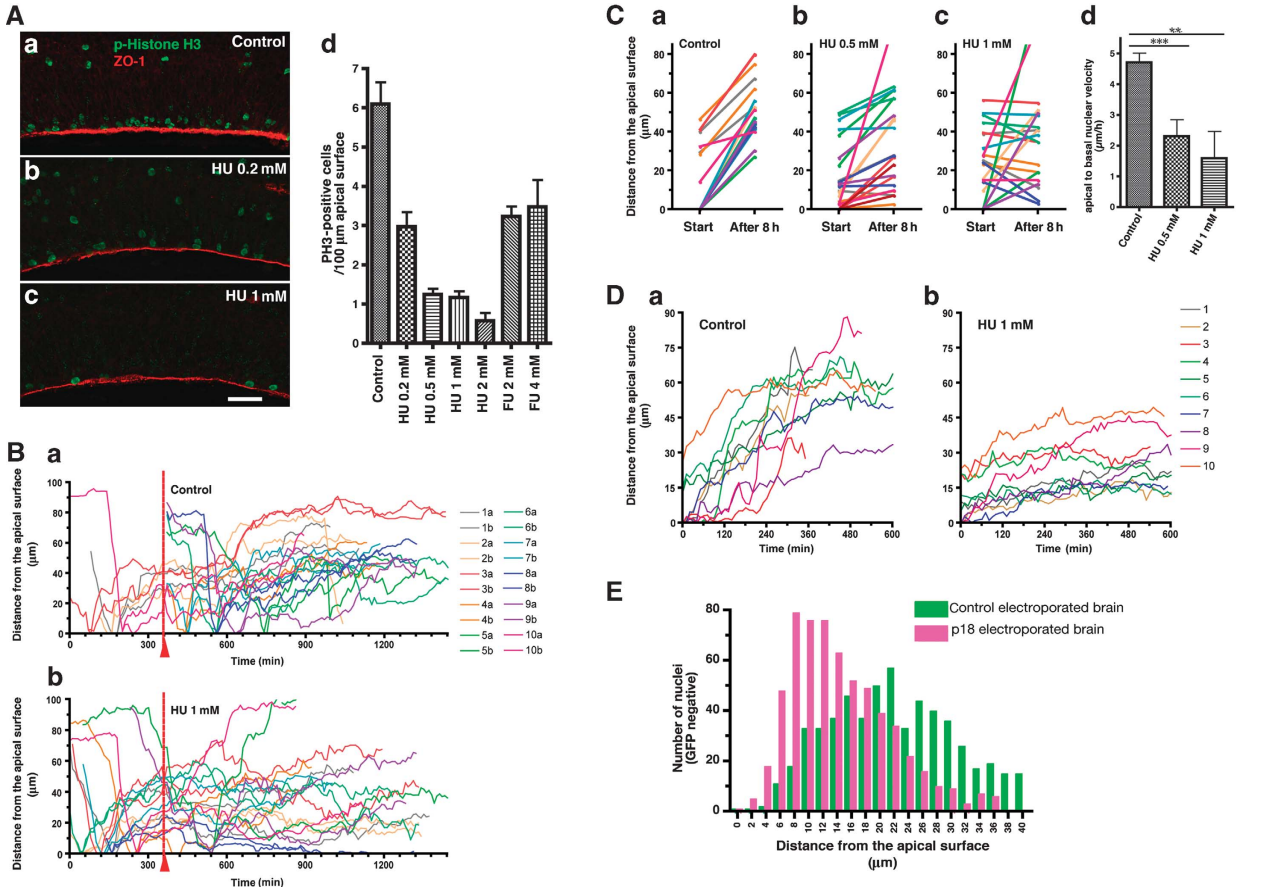

Figure 6 Cell-cycle arrest in S-phase perturbs apical-to-basal nuclear movement of neural progenitor cells in G1-phase. (**A**) Assessment of drug conditions that inhibit S-phase of neural progenitor cells in slice cultures prepared from E13.5 mouse brain tissue. (a–c) Immunostaining of cryosections prepared from brain slices after drug treatment. Concentrations of HU are indicated in the panels. Green, phosphorylated Histone H3 (mitotic cells); red, ZO-1 (apical surface). Bar = 50 μm. (d) M-phase neural progenitor cells in cultured slices after drug treatment. The average number of mitotic cells per 100 μm of apical surface under several conditions are indicated. Note that HU resulted in a concentration-dependent reduction of M-phase neural progenitor cells. FU, 5-fluorouracil. (**B**) Tracking of nuclear movements in brain slice cultures with HU treatment. Nuclei of neural progenitor cells were marked with NLS-GFP, and their distances from the apical surface (*y*-coordinate) were plotted versus their incubation time (*x*-coordinate). Red arrowheads indicate the time point when control vehicle (a) or 1 mM HU (b) was added to the medium (6 h after incubation started). Numbers and colour codes of nuclei are indicated on the right (a or b after the numbers indicates daughter cells derived from cell division at the apical surface). (**C**) Apical-to-basal nuclear movements following cell division at the apical surface during 8 h of incubation after adding (a) control vehicle, (b) 0.5 mM HU or (c) 1 mM HU. Colour codes are explained above. (d) Average velocities of nuclei are shown in (a–c) (20–22 cases in each condition). $^{**}P<0.005$, $^{***}P<0.001$, *t*-test. Error bars indicate s.e.m. (**D**) Effect of HU treatment on microbead movement induced from the apical surface. Positions of fluorescent beads relative to the apical surface (*y*-coordinate) were measured at each time point (*x*-coordinate) from time-lapse images. Six hours after adding microbeads to the brain slice cultures, control vehicle (a) or 1 mM HU (b) was added to the medium (indicated as time point 0). Tracked movements of 10 microbeads in each condition are displayed. (**E**) Effect of co-existing G1-arrested cells on the basally oriented nuclear movement of non-arrested cells. After *in utero* electroporation of plasmids of $p18^{Ink4c}$ and NLS-GFP into the E13.5 mouse brain, two thymidine analogues (CldU and IdU) were introduced into pregnant mice at different times (5 and 2 h, respectively) before fixing the embryos. With this procedure, CldU single-labelled cells were identified as having been in S-phase 2–5 h before fixation. During this time window, CldU single-labelled cells reach the apical surface, therefore their distribution pattern indicates nuclear position of late M-phase or G1-phase cells. Nuclei of $p18^{Ink4c}$ plasmid-negative cells were identified by the absence of NLS-GFP signals, and their position from the apical surface was measured. Histogram shows the comparison of the GFP-negative CldU single-labelled nuclear positions of six electroporated brains from three independent experiments (total number of measured nuclei; control $n = 550$, $p18^{Ink4c}$ $n = 594$).

Computational modelling displays non-autonomous nuclear migration

To evaluate the possibility that apical-to-basal nuclear migration occurs as a result of the displacement of nuclei in the apical VZ, we constructed a computational model for INM, and qualitatively compared the outcomes predicted by the model with the experimental data. To approximate the VZ occupied by nuclei, we designed a simplified two-dimensional model in which nuclei are represented as circles in a planar VZ constrained in the radial, but not lateral, direction. Basic rules were set for nuclei to move in the VZ to avoid neighbouring nuclei (Figure 7Aa): (1) A searching radius (SR) around each nucleus was assumed. (2) Each nucleus searches the area of the SR and then goes to the centre of gravity of an area within the SR that is unoccupied by nuclei. (3) The cell-cycle phase of each nucleus has a randomly provided initial value (colour codes are indicated in Figure 7Ab); the lengths of the cell-cycle phases were taken from values that have been experimentally measured in the developing mouse brain (Takahashi *et al*, 1995). If no commands are provided to

move nuclei, no nuclei move from their original positions (Figure 7Ba). In contrast, when G2- and M-phase nuclei are programmed to migrate in the basal-to-apical direction at 1.0 μm/min (an estimate from experimental results (Figures 1B and 3Ga)), all G1-phase and S-phase nuclei move in the apical-to-basal direction (Figure 7Bb; Supplementary Movie S11). We found remarkable similarities between the nuclear movements predicted by the computational model and those observed in brain slice cultures (Figure 1B). First, apical-to-basal nuclear migration is not linear, but shows back-and-forth

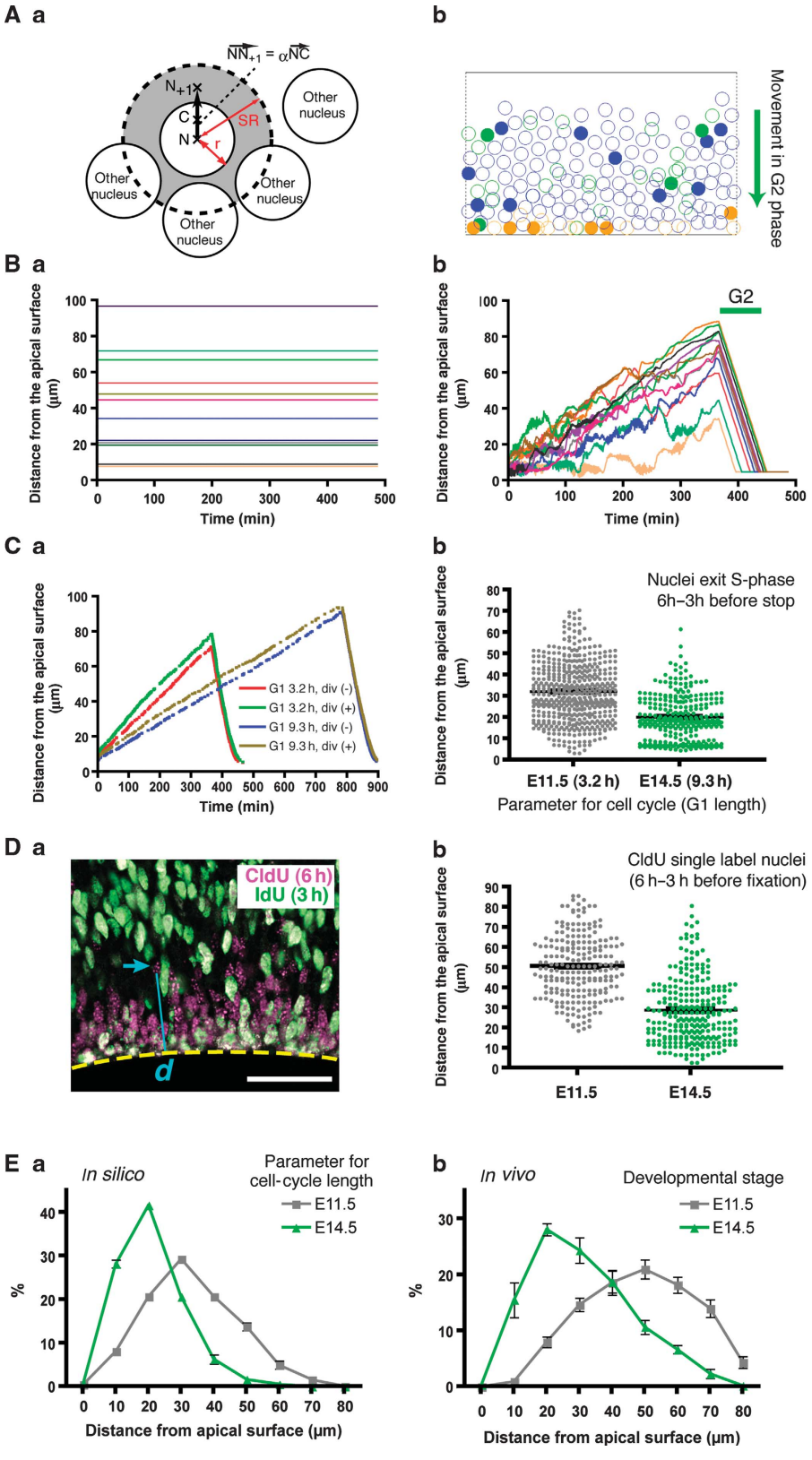

movement patterns. Second, the end position of the apical-to-basal migration varies significantly from nucleus to nucleus. This suggests that the conditions of the model are essentially consistent with the *in vivo* situation.

We used this computational model to identify conditions that significantly influence apical-to-basal migration by executing models with varying parameters. We found that changes in cell-cycle length had major effects on the velocity of apical-to-basal movement (Figure 7Ca). To further evaluate the validity of the computational model, we tested this prediction in brain tissue. The cell cycle of neural progenitors, particularly the duration of the G1-phase, becomes progressively longer as development progresses (Takahashi *et al*, 1995). Thus, the effect of cell-cycle length can be tested *in vivo* by comparing two different developmental stages. To compare results from the computational model with *in vivo* results using the same criteria, we designed *in silico* experiments to label the S-phase nuclei and measure the distance the nuclei move after exiting S-phase. We ran the program using the cell-cycle length parameters of E11.5 and E14.5 cells that were measured in a previous study (Takahashi *et al*, 1995). The positions of nuclei that were modelled as having exited S-phase 3–6 h earlier before the end of the simulation were plotted (Figure 7Cb). The average position of such nuclei was more distant from the apical surface when the cell-cycle length was shorter (E11.5). This result can be explained as occurring because a shorter cell cycle increases the frequency of basal-to-apical nuclear migration that occurs once in a cell cycle, resulting in more frequent displacements by G2 nuclei in the apical VZ. For *in vivo* experiments, we injected two thymidine analogues (CldU and IdU) into pregnant mice at different times (6 and 3 h, respectively) before fixation of the embryos. With this procedure, CldU single-labelled cells can be identified as having been in S-phase 3–6 h before fixation. As we did in the *in silico* experiments, we measured and plotted the distance of the CldU single-labelled nuclei from the apical surface at each stage (Figure 7Da and b). Histograms showing the distribution of nuclear positions indicate that the peak of the distribution was in the middle of the VZ at E11.5 but that it shifted significantly closer to the apical surface and showed a narrower distribution by E14.5 in both the model (Figure 7Ea) and in the developing brain (Figure 7Eb) (for the statistical test, see the Supplementary data). This qualitative correlation supports a model in which apical-to-basal nuclear migration is mainly driven by the displacement of nuclear migration in the basal-to-apical direction during G2-phase.

Discussion

In this study, we focused on how the timing and direction of INM are determined with respect to the cell cycle in neural progenitor cells. Our results indicate that there are different modes of nuclear migration depending on the phase of the cell cycle; active migration occurs during G2-phase, and passive migration during G1-phase. Several lines of evidence have suggested that the dynein motor system drives nuclei from the basal region toward the centrosome on the apical surface of the VZ (Tsai *et al*, 2005; Tamai *et al*, 2007; Xie *et al*, 2007; Del Bene *et al*, 2008), and that the connection between dynein and the nuclear envelope is maintained by SUN-domain proteins and KASH-domain proteins (Del Bene *et al*, 2008; Zhang *et al*, 2009). As their loss-of-function results in defects in INM and post-mitotic neuronal migration (Tsai *et al*, 2005; Zhang *et al*, 2009), these molecules appear to be part of ubiquitous machineries for microtubule-based nucleokinesis. Therefore, no specific molecular mechanism has so far been shown to link nuclear migration to cell-cycle progression. Here, we have demonstrated that cell-cycle progression from G1- to S-phase is a prerequisite for basal-to-apical nuclear migration, and that Tpx2 regulates this migration. Tpx2 begins to be expressed in S-phase and accumulates in the nucleus. Upon entry into G2-phase, Tpx2 redistributes into the apical process and promotes nuclear migration. In *Arabidopsis*, a similar translocation of Tpx2 from the nucleus to the prospindle prior to nuclear envelope breakdown has been identified (Vos *et al*, 2008). Our results thus suggest that translocation of nuclear Tpx2 to the apical process upon entry into G2-phase is critical for the microtubule-dynein-driven nuclear migration that occurs during G2-phase, while other molecules discussed above might be needed for Tpx2 to function in nuclear migration to the apical surface. We propose that the regulation of Tpx2 distribution is part of the mechanism that determines the timing of basal-to-apical nuclear migration.

How does Tpx2 function in nuclear migration in the apical process during G2-phase? Tpx2 is known to act in mitotic spindle organization at M-phase by controlling aurora A kinase (Barr and Gergely, 2007). Aurora A, in turn, activates transforming acid coiled-coil protein (TACC), which promotes microtubule extension from centrosomes (Kinoshita *et al*,

Figure 7 Computational modelling of INM combined with *in vivo* experiments. (**A**) (a) Scheme of nuclear movement posited in the model. The nucleus goes to the centre of gravity of an area that is unoccupied by neighbouring nuclei within the SR. r, radius of nucleus; SR, searching radius. (b) One of the frames from the sequential movie of modelling analyses visualized for interpretations (see Supplementary Movie S11). Some nuclei are highlighted by colour codes according to their phase in the cell cycle: blue, G1/S; green, G2; orange, M. Nuclei can cross the border of the lateral and basal sides but not that of the apical side. See details in Supplementary data. (**B**) Movement of 12 individual nuclei acquired from the computational model without (a) or with (b) basal-to-apical nuclear movement during G2-phase. *x*-coordinate: time, *y*-coordinate: distance from the apical surface. Note that the patterns of apical-to-basal movement and the points reached before entering G2-phase differ significantly among nuclei (b). (**C**) (a) Effect of changing parameters in the computational model. Average distances from the apical surface of 200 nuclei and their phase in the cell cycle in the simulation were plotted. Length of G1-phase in E11.5 (3.2 h) and E14.5 (9.3 h) and whether cell division at M-phase is occurring (+ or −) are indicated. (b) Relative positions of nuclei that exited S-phase between 3–6 h before the end of the simulation using the cell-cycle parameters for E11.5 (grey) or E14.5 (green). (**D**) (a) Incorporation of CldU (magenta) and IdU (green) into the nuclei of neural progenitor cells of mouse brains 6 and 3 h before fixation, respectively. Blue arrow: the presence of a CldU single-labelled nucleus implies that it exited S-phase between 6 and 3 h before fixation. Distance from the apical surface (yellow dashed line) was measured (d). Bar = 50 μm. (b) Positions of nuclei that exited S-phase between 6 and 3 h before fixation in E11.5 (grey) and E14.5 (green) embryonic mouse brains. (**E**) Histogram view of the results of the double-labelling experiment acquired from the computational model (a, see (**C**)) or *in vivo* mouse brains (b, see (**D**)). Proportions of nuclei (*x*-coordinate) at specific distances from the apical surface (*y*-coordinate, rounded off to a two-digit number).

2005). In this cascade, the absence of Tpx2 might result in the aberrant localization of TACC (Barr and Gergely, 2007). Although centrosomal proteins are known to be involved in INM (Xie *et al*, 2007), we observed that the loss of Tpx2 function did not affect the localization of TACC3 protein at the centrosome during mitosis (Supplementary Figure S5E), suggesting that Tpx2 can act independently of centrosomal proteins. We instead found that microtubule distribution in the apical process becomes narrower in width in the G2-phase compared with the G1-phase and that this change depends on Tpx2 function. Considering the *in vitro* activity of Tpx2 in promoting microtubule bundling (Schatz *et al*, 2003) and Tpx2 functions in the organization of the microtubule cytoskeleton in the apical process of neural progenitor cells *in vivo* (Figure 4), how such organized microtubules promote nuclear migration in the apical process remains to be elucidated. Interestingly, an *in vitro* study shows that dynein-dynactin-coated microbeads are less likely to pass microtubule–microtubule intersections than to switch from one microtubule to another (Ross *et al*, 2008). This result indicates that dynein-dependent motor activity carries organelles more efficiently in cases where microtubules are uniformly orientated. Microtubules may be more randomly orientated in the absence of the bundling activity of Tpx2, as occurs in G1-phase or in Tpx2-knockdown cells. Thus, the alignment of microtubules by Tpx2 could possibly enhance the function of the microtubule-dynein system, accounting for efficient nuclear migration in the apical process.

The most remarkable finding of this study is that nuclear migration in the apical-to-basal direction during G1-phase involves a passive, non-autonomous process dependent on the migration of nuclei during G2-phase, which takes place toward the apical surface and results in a higher nuclear density in the apical region and a lower nuclear density in the basal region of the VZ. In a packed tissue such as the VZ of the embryonic brain, free, mobile nuclei redistribute so that the nuclear density becomes homogeneous. Based on our experimental results and computational modelling, we propose a displacement model of INM, in which, after mitosis, nuclei on the ventricular surface are driven away from this surface by a collective displacement effect generated by other nuclei migrating toward the ventricular surface. This scenario is supported by the recently reported observation in zebrafish retina, suggesting that apical-to-basal nuclear movement during INM is a stochastic event (Norden *et al*, 2009). This does not mean that active, autonomous mechanisms are not involved in the apical-to-basal movement, but indicates a close link between migrations in two opposite directions, which is compatible with motor-dependent autonomous mechanisms in the movement in this direction. Recent work reported that kinesin-type microtubule plus-end-directed motors have a certain role in carrying the nucleus from the apical region to the basal region of the VZ (Tsai *et al*, 2010). Alternatively, it is demonstrated that myosin II is required for nuclear migration in the apical-to-basal direction (Schenk *et al*, 2009). However, another report documents that actomyosin drives the nucleus from the basal to the apical surface in zebrafish retina (Norden *et al*, 2009). A simple explanation for the obvious contradiction between those two studies is that involvement of the actomyosin system in the INM is not direction specific but rather is used to maintain general nucleokinesis. It is, however, also reported that inhibition of myosin II does not show any effect on INM (Tsai *et al*, 2010). Although the idea that microtubule- and actomyosin motors show coordinated operation in INM is attractive, further investigations are required to identify molecules that may control the direction and the cell-cycle dependency of actomyosin systems.

Our model proposed here for INM of neural progenitor cells not only explains how nuclear migration is associated with the cell cycle but also manifests a robust system capable of maintaining neuroepithelial architecture during development. Prior to and during the neurogenic period, neural progenitor cells expand their numbers by self-renewing divisions. Given that most mitoses of self-renewing neural progenitor cells take place at the apical surface throughout brain development (Kowalczyk *et al*, 2009), it would be advantageous for daughter cells to leave the mitotic area until their next mitosis, as this would increase the efficiency of mitosis in the region of the ventricular surface. According to our model, only two phases of INM are motor dependent, active processes: nuclear migration toward the ventricular surface and mitosis. During the remaining phases of INM, G1- and S-phase, the distribution of nuclei is non-autonomously determined by the positions of other nuclei. The G1- and S-phases of the cell cycle therefore operate as adjustable phases in INM that allow nuclei in the VZ to be dynamically arranged as a whole to minimize the imbalance in nuclear density and avoid disorder in the neuroepithelium.

The idea that INM might be related to the process of cell fate determination of neural progenitor cells in the developing brain is attractive (Latasa *et al*, 2009). Studies of mouse brain and zebrafish retina indicate that perturbation of INM by downregulation of centrosomal and microtubule motor-associated proteins, respectively, caused enhanced neurogenesis at the expense of neural progenitor cells (Xie *et al*, 2007; Del Bene *et al*, 2008). In a recent study, it was reported that neural progenitor cells of mice genetically deficient for SUN-domain and KASH-domain proteins show a proliferation defect (Zhang *et al*, 2009). Given that INM has a role in the cell fate decisions of neural progenitor cells, it is important to determine which phase of migration is crucial and what molecules are involved in cell fate choice. Our study suggests that autonomous nuclear movement toward the apical region affects migration in both directions. This implies that the rate of neurogenesis can be affected during INM in both directions. Del Bene *et al* (2008) proposed that perturbation of INM alters the rate of exposure of cells to Notch signalling, leading to premature neurogenesis. This study suggested that Notch becomes activated as nuclei move toward the apical surface, whereas it is downregulated as cells move in the opposite direction (Del Bene *et al*, 2008). In the mouse cortex, however, Notch-active nuclei are found in the basal region of the VZ (Tokunaga *et al*, 2004; Kawaguchi *et al*, 2008). Further studies are necessary to clarify how Notch signals are transduced during INM progression. From a mechanistic perspective, the role of centrosomes in INM is noteworthy. A close relationship between neurogenesis and centrosomal functions is suggested from the identification of causative genes of human autosomal-recessive primary microcephaly (MCPH genes; several MCPH genes, such as ASPM, CDK5rap2 and CENPJ, encode centrosomal proteins (Thornton and Woods, 2009)). It would be interesting to examine whether mutations in these genes result in defective INM in addition to their effect on mitotic cells, thus leading to impaired neurogenesis.

Materials and methods

Animals

All animal manipulations were performed in accordance with the guidelines for animal experiments at the RIKEN Centre for Developmental Biology.

DNA constructs and RNAi

CCPM (GE Healthcare) and EB3-tagRFP vector (Evrogen) were purchased. Other mammalian expression vectors were based on pCAGGS (Niwa *et al*, 1991). NLS-GFP was constructed by inserting oligonucleotides for three copies of a nuclear localization sequence (NLS) into EGFP-C1 (Clontech). For GFP-TPX2, full-length mouse *TPX2*-coding sequence was amplified from RIKEN FANTOM cDNA (Accession No. AK090101) and ligated into pCAG-EGFP-C1. For 6myc-TPX2, the GFP sequence in the plasmid above was substituted with six copies of the myc epitope sequence. For $p18^{Ink4c}$ expression, mouse $p18^{Ink4c}$-coding sequence was amplified from Mammalian Gene Collection cDNA (Accession No. BC027026) and ligated into pCAGGS (constructed by Dr Konno, RIKEN CDB). To knockdown *TPX2* by vector-type RNAi, the BLOCK-iT Pol II miR RNAi Expression Vector Kit (Invitrogen) was used (RNAi-target sequences: for *LacZ*, 5′-AAATCGCTGATTTGTGTAGTC-3′, and for *TPX2*, 5′-TAATGATAGTGCATCCTCTGG-3′). To enhance RNAi efficiency, the plasmid was modified to have four copies of the target sequence in tandem, then cloned into pCAGGS. To knockdown *TPX2* with double-stranded RNA, StealthRNAi (Invitrogen) (5′-AAGUGUUGUCAACUGCCUUCAACGG-3′) was electroporated into E12.5 mouse brain at a concentration of 50 μM in physiological saline solution.

Antibodies

The primary antibodies used were Tpx2 (rabbit, Santa Cruz; 1:50), BrdU (rat, Abcam; 1:300), GFP (chick, Aves Labs; 1:500), myc (mouse, Upstate; 1:100), Par-3 (rabbit, Upstate; 1:250), ZO-1 (mouse, Zymed; 1:100), β-catenin (mouse, BD; 1:1000), γ-tubulin (mouse, Sigma; 1:100), TACC3 (rabbit, 1:300) (Yao *et al*, 2007), Ki67 (mouse, Novocastra; 1:100), $p18^{Ink4c}$ (rabbit, Santa Cruz; 1:50), Tuj1 (mouse, Covance; 1:600), Tuj1 (rabbit, Covance; 1:500), PCNA (mouse, BD; 1:100), mouse mAb against phospho-Histone H3 (pH 3) (mouse, Sigma; 1:100), pH 3 (rabbit, Upstate; 1:500), Pax6 (rabbit, Chemicon; 1:300), Sox2 (rabbit, Chemicon; 1:500), α-tubulin (rat, Serotec; 1:500) and Tbr2 (rabbit, Abcam; 1:100). To recognize CldU and IdU, BrdU (rat, Abcam; 1:300) and BrdU (mouse, BD; 1:50) were used, respectively.

Brain slice culture and incorporation of fluorescent microbeads

Coronal brain tissue slices were prepared from ICR mice and cultured in collagen gels as described previously (Miyata *et al*, 2001) with slight modifications. For details, see the Supplementary data.

Time-lapse imaging analysis

Time-lapse images of the movements of NLS-GFP-containing nuclei and fluorescent beads in embryonic mouse brain slice cultures are described in the Supplementary data.

Computational modelling

Construction of the two-dimensional model to evaluate the displacement effect for INM, and the effect of parameter settings, are described in Supplementary data.

Supplementary data

Supplementary data are available at *The EMBO Journal* Online (http://www.embojournal.org).

Acknowledgements

We thank Dr Shigenobu Yonemura and Kisa Kakiguchi (RIKEN CDB) for electron microscopy studies. HVEM observations at the National Institute of Physiological Sciences (NIPS) were performed under the instruction of Dr Tatsuo Arii (NIPS). We thank Drs Tetsuo Noda and Ryoji Yao (The Cancer Institute) for providing anti-TACC3 antibody. We thank Drs Raj Ladher and Guojun Sheng (RIKEN CDB) for critical reading of the manuscript. YMK was supported by Takeda Science Foundation.

Author contributions: YK and FM designed the project and wrote the manuscript. YK and TS performed most of the experiments and data analysis. AK designed and performed the computational modelling. KT and MS designed and performed electron microscopic analysis of microtubule organization. YMK designed live imaging of microtubule dynamics. SAB developed the tracking software.

Conflict of interest

The authors declare that they have no conflict of interest.

References

Barr AR, Gergely F (2007) Aurora-A: the maker and breaker of spindle poles. *J Cell Sci* **120:** 2987–2996

Bort R, Signore M, Tremblay K, Martinez Barbera JP, Zaret KS (2006) Hex homeobox gene controls the transition of the endoderm to a pseudostratified, cell emergent epithelium for liver bud development. *Dev Biol* **290:** 44–56

Cappello S, Attardo A, Wu X, Iwasato T, Itohara S, Wilsch-Brauninger M, Eilken HM, Rieger MA, Schroeder TT, Huttner WB, Brakebusch C, Götz M (2006) The Rho-GTPase cdc42 regulates neural progenitor fate at the apical surface. *Nat Neurosci* **9:** 1099–1107

Carneiro AC, Fragel-Madeira L, Silva-Neto MA, Linden R (2008) A role for CK2 upon interkinetic nuclear migration in the cell cycle of retinal progenitor cells. *Dev Neurobiol* **68:** 620–631

Del Bene F, Wehman AM, Link BA, Baier H (2008) Regulation of neurogenesis by interkinetic nuclear migration through an apical-basal notch gradient. *Cell* **134:** 1055–1065

Fujita S (1960) Mitotic pattern and histogenesis of the central nervous system. *Nature* **185:** 702–703

Götz M, Huttner WB (2005) The cell biology of neurogenesis. *Nat Rev Mol Cell Biol* **6:** 777–788

Götz M, Stoykova A, Gruss P (1998) Pax6 controls radial glia differentiation in the cerebral cortex. *Neuron* **21:** 1031–1044

Graham V, Khudyakov J, Ellis P, Pevny L (2003) SOX2 functions to maintain neural progenitor identity. *Neuron* **39:** 749–765

Gruss OJ, Carazo-Salas RE, Schatz CA, Guarguaglini G, Kast J, Wilm M, Le Bot N, Vernos I, Karsenti E, Mattaj IW (2001) Ran induces spindle assembly by reversing the inhibitory effect of importin alpha on TPX2 activity. *Cell* **104:** 83–93

Gruss OJ, Vernos I (2004) The mechanism of spindle assembly: functions of Ran and its target TPX2. *J Cell Biol* **166:** 949–955

Gruss OJ, Wittmann M, Yokoyama H, Pepperkok R, Kufer T, Sillje H, Karsenti E, Mattaj IW, Vernos I (2002) Chromosome-induced microtubule assembly mediated by TPX2 is required for spindle formation in HeLa cells. *Nat Cell Biol* **4:** 871–879

Guan KL, Jenkins CW, Li Y, Nichols MA, Wu X, O'Keefe CL, Matera AG, Xiong Y (1994) Growth suppression by p18, a p16INK4/MTS1- and p14INK4B/MTS2-related CDK6 inhibitor, correlates with wild-type pRb function. *Genes Dev* **8:** 2939–2952

Hayes NL, Nowakowski RS (2000) Exploiting the dynamics of S-phase tracers in developing brain: interkinetic nuclear migration for cells entering versus leaving the S-phase. *Dev Neurosci* **22:** 44–55

Kawaguchi D, Yoshimatsu T, Hozumi K, Gotoh Y (2008) Selection of differentiating cells by different levels of delta-like 1 among neural precursor cells in the developing mouse telencephalon. *Development* **135:** 3849–3858

Kinoshita K, Noetzel TL, Pelletier L, Mechtler K, Drechsel DN, Schwager A, Lee M, Raff JW, Hyman AA (2005) Aurora A phosphorylation of TACC3/maskin is required for centrosome-dependent microtubule assembly in mitosis. *J Cell Biol* **170:** 1047–1055

Kowalczyk T, Pontious A, Englund C, Daza RA, Bedogni F, Hodge R, Attardo A, Bell C, Huttner WB, Hevner RF (2009) Intermediate neuronal progenitors (Basal progenitors) produce pyramidal-projection neurons for all layers of cerebral cortex. *Cereb Cortex* **19:** 2439–2450

Latasa MJ, Cisneros E, Frade JM (2009) Cell cycle control of Notch signaling and the functional regionalization of the neuroepithelium during vertebrate neurogenesis. *Int J Dev Biol* **53:** 895–908

Machon O, van den Bout CJ, Backman M, Kemler R, Krauss S (2003) Role of beta-catenin in the developing cortical and hippocampal neuroepithelium. *Neuroscience* **122:** 129–143

Messier PE (1978) Microtubules, interkinetic nuclear migration and neurulation. *Experientia* **34:** 289–296

Messier PE, Auclair C (1974) Effect of cytochalasin B on interkinetic nuclear migration in the chick embryo. *Dev Biol* **36:** 218–223

Mimori-Kiyosue Y, Tsukita S (2003) 'Search-and-capture' of microtubules through plus-end-binding proteins (+TIPs). *J Biochem* **134:** 321–326

Minobe S, Sakakibara A, Ohdachi T, Kanda R, Kimura M, Nakatani S, Tadokoro R, Ochiai W, Nishizawa Y, Mizoguchi A, Kawauchi T, Miyata T (2009) Rac is involved in the interkinetic nuclear migration of cortical progenitor cells. *Neurosci Res* **63:** 294–301

Miyata T, Kawaguchi A, Okano H, Ogawa M (2001) Asymmetric inheritance of radial glial fibers by cortical neurons. *Neuron* **31:** 727–741

Murciano A, Zamora J, Lopez-Sanchez J, Frade JM (2002) Interkinetic nuclear movement may provide spatial clues to the regulation of neurogenesis. *Mol Cell Neurosci* **21:** 285–300

Niwa H, Yamamura K, Miyazaki J (1991) Efficient selection for high-expression transfectants with a novel eukaryotic vector. *Gene* **108:** 193–199

Norden C, Young S, Link BA, Harris WA (2009) Actomyosin is the main driver of interkinetic nuclear migration in the retina. *Cell* **138:** 1195–1208

Pearson RA, Luneborg NL, Becker DL, Mobbs P (2005) Gap junctions modulate interkinetic nuclear movement in retinal progenitor cells. *J Neurosci* **25:** 10803–10814

Raphael Y, Adler HJ, Wang Y, Finger PA (1994) Cell cycle of transdifferentiating supporting cells in the basilar papilla. *Hear Res* **80:** 53–63

Ross JL, Shuman H, Holzbaur EL, Goldman YE (2008) Kinesin and dynein-dynactin at intersecting microtubules: motor density affects dynein function. *Biophys J* **94:** 3115–3125

Sauer FC (1935) Mitosis in the neural tube. *J Comp Neurol* **62:** 377–405

Sauer ME, Walker BE (1959) Radioautographic study of interkinetic nuclear migration in the neural tube. *Proc Soc Exp Biol Med* **101:** 557–560

Schatz CA, Santarella R, Hoenger A, Karsenti E, Mattaj IW, Gruss OJ, Carazo-Salas RE (2003) Importin alpha-regulated nucleation of microtubules by TPX2. *EMBO J* **22:** 2060–2070

Schenk J, Wilsch-Brauninger M, Calegari F, Huttner WB (2009) Myosin II is required for interkinetic nuclear migration of neural progenitors. *Proc Natl Acad Sci USA* **106:** 16487–16492

Sherr CJ, Roberts JM (1999) CDK inhibitors: positive and negative regulators of G1-phase progression. *Genes Dev* **13:** 1501–1512

Takahashi T, Nowakowski RS, Caviness Jr VS (1992) BUdR as an S-phase marker for quantitative studies of cytokinetic behaviour in the murine cerebral ventricular zone. *J Neurocytol* **21:** 185–197

Takahashi T, Nowakowski RS, Caviness Jr VS (1993) Cell cycle parameters and patterns of nuclear movement in the neocortical proliferative zone of the fetal mouse. *J Neurosci* **13:** 820–833

Takahashi T, Nowakowski RS, Caviness Jr VS (1995) The cell cycle of the pseudostratified ventricular epithelium of the embryonic murine cerebral wall. *J Neurosci* **15:** 6046–6057

Tamai H, Shinohara H, Miyata T, Saito K, Nishizawa Y, Nomura T, Osumi N (2007) Pax6 transcription factor is required for the interkinetic nuclear movement of neuroepithelial cells. *Genes Cells* **12:** 983–996

Taverna E, Huttner WB (2010) Neural progenitor nuclei IN motion. *Neuron* **67:** 906–914

Thornton GK, Woods CG (2009) Primary microcephaly: do all roads lead to Rome? *Trends Genet* **25:** 501–510

Toida K, Kosaka K, Aika Y, Kosaka T (2000) Chemically defined neuron groups and their subpopulations in the glomerular layer of the rat main olfactory bulb—IV. Intraglomerular synapses of tyrosine hydroxylase-immunoreactive neurons. *Neuroscience* **101:** 11–17

Tokunaga A, Kohyama J, Yoshida T, Nakao K, Sawamoto K, Okano H (2004) Mapping spatio-temporal activation of Notch signaling during neurogenesis and gliogenesis in the developing mouse brain. *J Neurochem* **90:** 142–154

Tsai JW, Bremner KH, Vallee RB (2007) Dual subcellular roles for LIS1 and dynein in radial neuronal migration in live brain tissue. *Nat Neurosci* **10:** 970–979

Tsai JW, Chen Y, Kriegstein AR, Vallee RB (2005) LIS1 RNA interference blocks neural stem cell division, morphogenesis, and motility at multiple stages. *J Cell Biol* **170:** 935–945

Tsai JW, Lian WN, Kemal S, Kriegstein AR, Vallee RB (2010) Kinesin 3 and cytoplasmic dynein mediate interkinetic nuclear migration in neural stem cells. *Nat Neurosci* **13:** 1463–1471

Tsuda S, Kitagawa T, Takashima S, Asakawa S, Shimizu N, Mitani H, Shima A, Tsutsumi M, Hori H, Naruse K, Ishikawa Y, Takeda H (2010) FAK-mediated extracellular signals are essential for interkinetic nuclear migration and planar divisions in the neuroepithelium. *J Cell Sci* **123:** 484–496

Ueno M, Katayama K, Yamauchi H, Nakayama H, Doi K (2006) Cell cycle progression is required for nuclear migration of neural progenitor cells. *Brain Res* **1088:** 57–67

Vos JW, Pieuchot L, Evrard JL, Janski N, Bergdoll M, de Ronde D, Perez LH, Sardon T, Vernos I, Schmit AC (2008) The plant TPX2 protein regulates prospindle assembly before nuclear envelope breakdown. *Plant Cell* **20:** 2783–2797

Wright JA, Chan AK, Choy BK, Hurta RA, McClarty GA, Tagger AY (1990) Regulation and drug resistance mechanisms of mammalian ribonucleotide reductase, and the significance to DNA synthesis. *Biochem Cell Biol* **68:** 1364–1371

Xie Z, Moy LY, Sanada K, Zhou Y, Buchman JJ, Tsai LH (2007) Cep120 and TACCs control interkinetic nuclear migration and the neural progenitor pool. *Neuron* **56:** 79–93

Yao R, Natsume Y, Noda T (2007) TACC3 is required for the proper mitosis of sclerotome mesenchymal cells during formation of the axial skeleton. *Cancer Sci* **98:** 555–562

Zhang X, Lei K, Yuan X, Wu X, Zhuang Y, Xu T, Xu R, Han M (2009) SUN1/2 and Syne/Nesprin-1/2 complexes connect centrosome to the nucleus during neurogenesis and neuronal migration in mice. *Neuron* **64:** 173–187